VIETNAM ACADEMY OF SCIENCE AND TECHNOLOGY

Vietnam Journal of MECHANICS

Volume 35 Number 3

ISSN 0866-7136

VN INDEX 12.666

3
2013
35th Anniversary

Vietnam Journal of Mechanics, VAST, Vol. 35, No. 3 (2013), pp. 225 – 237

ON TWO-FIELD NURBS-BASED ISOGEOMETRIC FORMULATION FOR INCOMPRESSIBLE MEDIA PROBLEMS

Tran Vinh Loc[1], **Thai Hoang Chien**[1], **Nguyen Xuan Hung**[1,2,*]
[1] *Ton Duc Thang University, Ho Chi Minh City, Vietnam*
[2] *University of Science, VNU-HCMC, Ho Chi Minh City, Vietnam*
[*]E-mail: nxhung@hcmus.edu.vn

Abstract. This paper presents **u**-p mixed formulation relied on the framework of NURBS-based Isogeometric approach (IgA) for incompressible problems. In mixed method, displacement (velocity) field is approximated using NURBS basis functions with one order higher than that of pressure one. Being different from the standard FEM, the IgA allows to increase (or decrease) easily the order and continuous derivative of interpolated functions. As a result, a family of NURBS elements, which satisfies the inf-sup condition, is obtained. Benchmark examples are given to validate the excellent performance of the method.

Keywords: NURBS, isogeometric, inf-sup, volumetric locking, mixed formulation.

1. INTRODUCTION

In computational mechanics, almost of materials are characterized by Young's modulus E and Poisson's ratio ν. While Young's modulus is a measure of the stiffness of an elastic material, Poisson's ratio ν is defined as the ratio of the lateral compression to the expansion. Mathematically, when ν equals 0.5 the bulk modulus λ is infinitive, so the system of equilibrium equation becomes highly ill-condition and therefore the accuracy of solution is lost when using lower order finite elements. This phenomenon is called volumetric locking and materials which have $\nu \approx 0.5$ are called incompressible materials. Some examples of incompressible or nearly incompressible materials are rubber elasticity, metal plasticity, incompressible flow, etc.

To overcome volumetric locking problem, numerous studies have been devised, for example, mixed formulation [1, 2], enhanced assumed strain (EAS) modes [3], reduced integration stabilizations [4], average node technique [5], meshfree methods [6, 7], etc. Among them, **u**-p mixed formulation is found to be very popular approach. This approach was firstly introduced by Chorin [8] who solved incompressible viscous flow problem with two fields: pressure and displacement fields which are approximated independently. However, when using approximation fields with linear interpolation, the Ladyzhenskaya-Babuska-Brezzi (LBB) inf-sup condition is not fulfilled [1]. To overcome this shortcoming, Arnold

et al. proposed a so-called MINI element [9] which still uses linear elements with enrichment of cubic bubble functions. However, such the method uses the discretized geometry through mesh generation. This process often leads to the geometrical error. Also, the communication of geometry model and mesh generation during analysis process in order to provide the desired accuracy of solution is always needed and this consumes much time [10], especially for industrial problems.

Hughes et al. [10] have recently proposed a new computational method so-called Isogeometric Analysis (IGA) to closely link the gap between Computer Aided Design (CAD) and Finite Element Analysis (FEA). It means that the IGA uses the same basis functions to describe both the geometry of domain (CAD) and the approximate solution. Being different from interpolated functions of the standard FEM based on Lagrange polynomial, Isogeometric approach utilizes more general basis functions such as B-splines and Non-Uniform Rational B-splines (NURBS) that are common in CAD geometry. The exact geometry is therefore maintained at the coarsest level of discretization and the re-meshing is performed on this coarsest level without any communication with CAD geometry. Furthermore, B-splines (or NURBS) provide a flexible way to make refinement, de-refinement, and degree elevation [11]. They allow us to easily achieve the smoothness with arbitrary continuity order compared to the traditional FEM. With many advantages, in recent years IGA has been extensively studied for nearly incompressible linear and non-linear elasticity and plasticity problem [12], steady-state incompressible Stoke problems in the benchmarking lid-driven square cavity [13], two dimensional steady-state Navier-Stokes flow [14], etc.

In this paper, we promote a family of **u**-p mixed elements based on the Isogeometric method for incompressible media problems. In **u**-p mixed elements, displacement field (velocity) is approximated using NURBS basis functions with one order higher than that of pressure one. As a result, a family of NURBS elements verifies the inf-sup condition. The method allows one to increase (or decrease) easily the order and continuous derivative of interpolated functions. Some benchmark problems are provided to demonstrate the reliability and effectiveness of the present method.

The paper is outlined as follows: in the next section the finite mixed displacement – pressure form is briefed. A formulation of Isogeometric analysis is presented in section 3. Section 4 devotes some numerical examples. Section 5 closes some remarking conclusions.

2. BRIEF ON THE FINITE MIXED DISPLACEMENT-PRESSURE FORM

2.1. Mixed displacement – pressure form

Let consider a solid body defined in a domain Ω with a Lipschitz continuous boundary Γ such that $\Gamma = \Gamma_u \cup \Gamma_t, \Gamma_u \cap \Gamma_t = \emptyset$ where Γ_u, Γ_t are Dirichlet and Neumann boundary, respectively. A body force **b** acts within the domain. The mixed displacement – pressure form is governed by

$$\nabla . \boldsymbol{\sigma} + \mathbf{b} = 0 \text{ in } \Omega \tag{1}$$

$$\nabla . \mathbf{u} - \frac{p_r}{\lambda} = 0 \text{ in } \Omega \tag{2}$$

and needs to satisfy on Dirichlet and Neumann boundary conditions

$$\mathbf{u} = \bar{\mathbf{u}} \quad \text{on} \quad \Gamma_u \tag{3}$$

$$\boldsymbol{\sigma} \,.\, \mathbf{n} \,=\, \bar{\mathbf{t}} \quad \text{on} \quad \Gamma_t \tag{4}$$

The stress field is split into two parts: the deviatoric stress $\mathbf{s}$ and the pressure p_r

$$\boldsymbol{\sigma}(\mathbf{u}, p_r) \;=\; \mathbf{s} \,+\, p_r \mathbf{m} \,=\, \mu \mathbf{D}_{dev}\, \boldsymbol{\varepsilon}(\mathbf{u}) + p_r \mathbf{m} \tag{5}$$

where $\mathbf{m} = [\,1\;1\;0\,]^T$, $\mu = E/2(1+\nu)$, $\lambda = E/3(1-2\nu)$ are Lame parameters of solid and $\mu \mathbf{D}_{dev}$ is the deviatoric projection of the elastic matrix $\mathbf{D}$ given by

$$\mathbf{D}_{dev} = \frac{1}{3} \begin{bmatrix} 4 & -2 & 0 \\ -2 & 4 & 0 \\ 0 & 0 & 3 \end{bmatrix} \tag{6}$$

and the compatibility relation between strain $\boldsymbol{\varepsilon}$ and displacement field $\mathbf{u}$

$$\boldsymbol{\varepsilon} \,=\, \boldsymbol{\partial} \mathbf{u} \quad \text{where} \quad \boldsymbol{\partial} = \begin{bmatrix} \partial/\partial x & 0 & \partial/\partial y \\ 0 & \partial/\partial y & \partial/\partial x \end{bmatrix}^T \tag{7}$$

2.2. Weak form

The mixed approach finds a displacement field $\mathbf{u} \in \mathbb{V}_0 \subset \mathbb{H}_0^1(\Omega)^2$ and pressure $p_r \in \mathbb{P} \subset \mathbb{L}_0^2(\Omega)$ that satisfies the standard Galerkin weak form [1]

$$\begin{aligned} a(\mathbf{u}, \mathbf{v}) + b(p_r, \mathbf{v}) &= f(\mathbf{v}), \forall \mathbf{v} \in \mathbb{V}_0 \\ b(q, \mathbf{u}) - \frac{1}{\lambda}(p_r, q) &= 0, \forall q \in \mathbb{P} \end{aligned} \tag{8}$$

where bilinear forms $a(.,.), b(.,.)$ are defined as

$$\begin{aligned} a(\mathbf{u}, \mathbf{v}) &= 2\mu \int_\Omega \boldsymbol{\varepsilon}^T(\mathbf{u}) \mathbf{D}_{dev}\, \boldsymbol{\varepsilon}(\mathbf{v}) \mathrm{d}\Omega \\ b(q, \mathbf{u}) = \int_\Omega q(\nabla \cdot \mathbf{u}) \mathrm{d}\Omega, &\quad (q, p_r) = \int_\Omega q p_r \mathrm{d}\Omega \end{aligned} \tag{9}$$

and the linear form $f(.)$ is given by

$$f(\mathbf{v}) = \int_\Omega \mathbf{b}^T \mathbf{v} \mathrm{d}\Omega + \int_{\Gamma_t} \bar{\mathbf{t}}^T \mathbf{v} \mathrm{d}\Gamma \tag{10}$$

with $\nabla \cdot (\bullet)$ denotes divergence.

3. THE FORMULATION OF ISOGEOMETRIC APPROACH

3.1. B-spline and NURBS basis functions

To build a B-spline in one dimension, we firstly define two positive integers: a polynomial degree p and number of control point n and a knot vector $\boldsymbol{\Xi} = \{\xi_1, \xi_2, ..., \xi_{n+p+1}\}$ with parametric value $\xi_i \in [\,0\;1\,]$ where $i = 1, ..., n+p+1$.

We assume that all internal knots have multiplicity r times, $1 \le r \le p-1$, so that knot vector can be rewritten in the following form

$$\boldsymbol{\Xi} = \{\underbrace{\xi_1, ..., \xi_1}_{p+1 \text{ times}}, \underbrace{\xi_2, ..., \xi_2}_{r \text{ times}}, ..., \underbrace{\xi_m, ..., \xi_m}_{p+1 \text{ times}}\} \tag{11}$$

and the relation is $m = 2 + \dfrac{n-p-1}{r}$.

The B-spline basis functions $N_{i,p} : [\,0\ 1\,] \to \mathbb{R}$ are defined by the following recursion formula for $p = 0$ [10]

$$N_{i,0}(\xi) = \begin{cases} 1 & \text{if } \xi_i \le \xi < \xi_{i+1} \\ 0 & \text{otherwise} \end{cases} \tag{12}$$

and for $p \ge 1$

$$N_{i,p}(\xi) = \frac{\xi - \xi_i}{\xi_{i+p} - \xi_i} N_{i,p-1}(\xi) + \frac{\xi_{i+p+1} - \xi}{\xi_{i+p+1} - \xi_{i+1}} N_{i+1,p-1}(\xi) \tag{13}$$

The basis functions are piecewise polynomials of order p, but at ξ_i they have $k := p - r$ continuous derivatives.

Then, with the matrix of the control points $\mathbf{P}_i$ and the basis functions $N_{i,p}(\xi)$, the B-Spline curve is defined as

$$\mathbf{C}(\xi) = \sum_{i=1}^{n} N_{i,p}(\xi)\, \mathbf{P}_i \tag{14}$$

In two dimension, the B-Spline surface is evaluated by the tensor product of basis functions in two parametric dimensions ξ and η with two knot vectors $\boldsymbol{\Xi} = \{\xi_1, \xi_2, ..., \xi_{n+p+1}\}$ and $\mathrm{H} = \{\eta_1, \eta_2, ..., \eta_{m+q+1}\}$ is expressed as follows

$$\mathbf{S}(\xi, \eta) = \sum_{i=1}^{n} \sum_{j=1}^{m} N_{i,p}(\xi)\, M_{j,q}(\eta)\, \mathbf{P}_{i,j} \tag{15}$$

where $\mathbf{P}_{i,j}$ is the bidirectional control net, $N_{i,p}(\xi)$ and $M_{j,q}(\eta)$ are the B-spline basis functions defined on the knot vectors over an $m \times n$ net of control points $\mathbf{P}_{i,j}$.

Similarly notations used in finite elements, we identify the logical coordinates (i, j) of the B-spline surface with the traditional notation of a node A. Eq. (15) can be rewritten as

$$\mathbf{S}(\xi, \eta) = \sum_{A}^{m \times n} N_A(\xi, \eta)\, \mathbf{P}_A \tag{16}$$

where $N_A(\xi, \eta) = N_{i,p}(\xi)\, M_{j,q}(\eta)$ is the shape function associated with node A.

To present exactly some curved geometry, however, (e.g. circles, cylinders, spheres, etc.) non-uniform rational B-splines (NURBS) is used. Be different from B-spline, each control point of NURBS has additional value called an individual weight w_A. The weighting function is expressed as

$$w(\xi, \eta) = \sum_{A}^{m \times n} N_A(\xi, \eta)\, w_A \tag{17}$$

Then the NURBS surface can be defined as

$$\mathbf{S}(\xi, \eta) = \sum_{A=1}^{m \times n} R_A(\xi, \eta) \mathbf{P}_A \text{ with } R_A = \frac{N_A w_A}{w} \tag{18}$$

Fig. 1 gives an example about annular geometry which is constructed by isogeometric approach. Firstly, we determine two knot vectors $\boldsymbol{\Xi} = \{0,\ 0,\ 0,\ 1,\ 1,\ 1\}$ and $\mathrm{H} = \{0, 0, 1, 1\}$

Table 1. The coordinates and weight values of control points for the annular domain with internal and external radius equal 1 and 2, respectively.

I	1	2	3	4	5	6
x_i	2	2	0	1	1	0
y_i	0	2	2	0	1	1
w_i	1	$\sqrt{2}/2$	1	1	$\sqrt{2}/2$	1

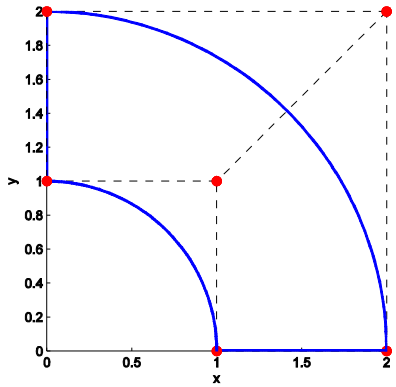

Fig. 1. Coarsest mesh (in blue colour) and control points (in red colour) of the annular domain

in tangential and radial dimensions, respectively and six control points (in red colour) with values given in Tab. 1. Then using (18), we can plot the domain in blue colour. Being more excellent than FEM, just with 6 points IGA models exactly the problem domain. Note that using the weight values being different from value 1, the control points need not to lie in the boundary of element as shown in Fig. 1.

3.2. Refinement technique

In computation, to reach the desired results, similar to other approximate methods, IGA also needs some refinement techniques such as h-refinement, p-refinement, k-refinement. Fig. 2 presents an example of h-refinement or so-called knot insertion. In this example, as the knot is inserted between two distinct knots $[\xi_i,\ \xi_{i+1}]$ the NURBS element increases. Fig. 3 shows k-refinement – a special technique only having in Isogeometric approach. From coarsest mesh with only one element in Fig. 1, applying h-refinement we can create a meshing with 2×4 NURBS elements in Fig. 2b. By repeating the first and the last values in knot vector, the polynomial order of basis functions is increased from $p = 2, 3, 4$.

In those above figures, the domain is described by the NURBS basis functions which have order p and maintain the continuity at p-1 level. Especially, in IGA, the continuity

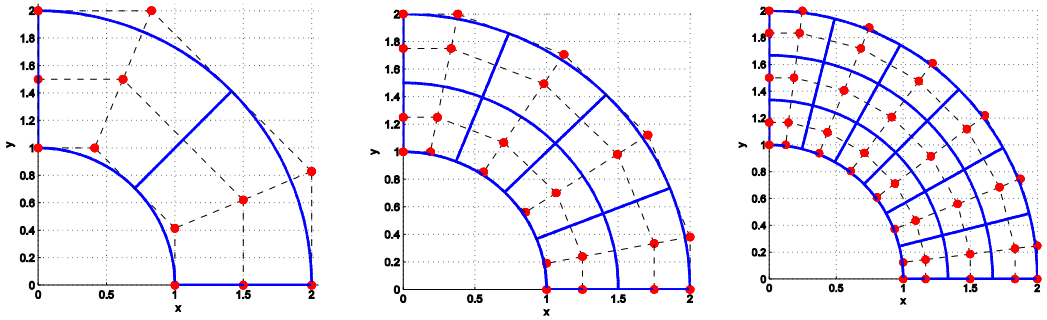

(a) (b) (c)

Fig. 2. Knot insertion

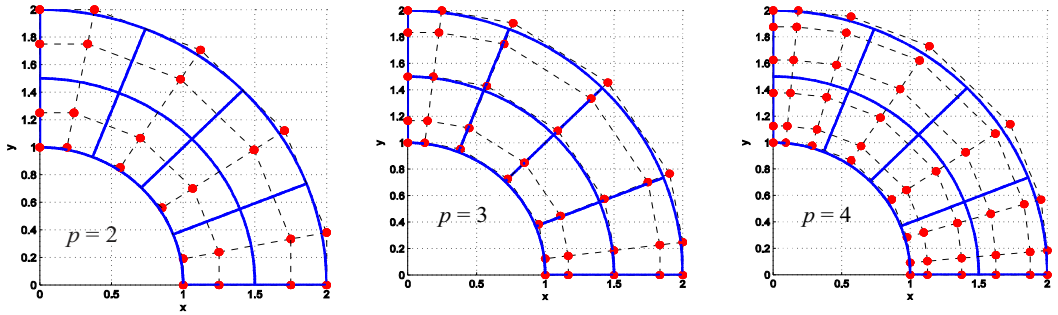

(a) (b) (c)

Fig. 3. Order elevation: the order of basis functions are increased from $p = 2$ to $p = 3, 4$

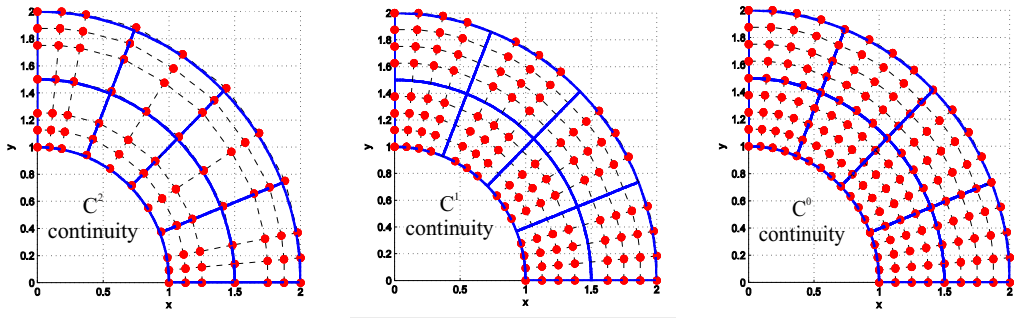

(a) (b) (c)

Fig. 4. The continuity element decreases according to C^{p-r}

can be controlled easily as shown in Fig. 4. It can be seen that as we repeat the internal distinct knot values r time, the order of continuity of NURBS element decreases following to value of $p - r$. Following this, the number of control points in each direction increases to $(n - p - 1)r + (p + 1)$.

3.3. Discrete weak form

In this mixed formulation, both of displacement (or velocity) and pressure are unknown variables. Displacements are discretized using NURBS basis functions with order p ($p \geq 2$)

$$\mathbf{u}^h = \sum_A^{n_u} R_A(\xi, \eta)\mathbf{u}_A \tag{19}$$

while the pressure field is approximated by NURBS basis functions with order p-1 being lower than that of displacements.

$$p_r^h = \sum_A^{n_p} P_A(\xi, \eta)p_A \tag{20}$$

where $\mathbf{u}_A, p_A$ is the vector of nodal displacements and pressure according to control point A, respectively, n_u, n_p are the number of control points need to be used to describe the displacement and pressure field, respectively, in each NURBS element. Their values rise based on the increment of order p, e.g, see Fig. 5.

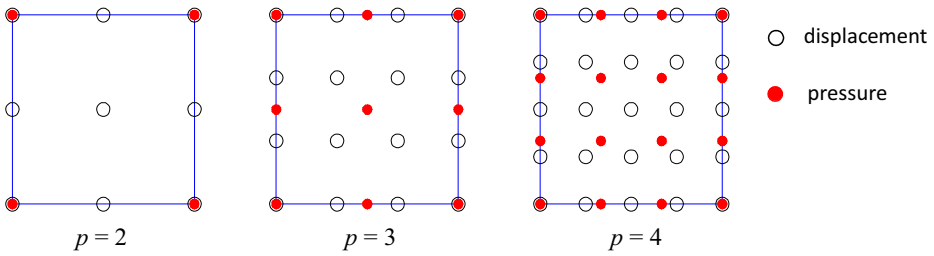

Fig. 5. C^0 continuity NURBS elements

In Fig. 5, the number of control points increase from 9 to 25 and from 4 to 16 for displacement and pressure description, respectively. Here, we just use C^0 continuity NURBS element, so some the control points lie on boundary of element. In our approach, because the displacement and pressure field are approximated independently the nodes for discretizing them do not need to overlap.

Substituting Eq. (19) into Eq. (7) the strain vector is rewritten as

$$\boldsymbol{\varepsilon}^h = \sum_A^{n_u} \mathbf{B}_A\mathbf{u}_A \tag{21}$$

where the strain matrix for node A

$$\mathbf{B}_A = \begin{bmatrix} R_{A,x} & 0 \\ 0 & R_{A,y} \\ R_{A,y} & R_{A,x} \end{bmatrix} \tag{22}$$

Substituting Eqs. (19), (20) and (21) into Eq. (8), the mixed approximation can be expressed in matrix form as

$$\begin{bmatrix} \mathbf{A} & \mathbf{G}' \\ \mathbf{G} & -\mathbf{V} \end{bmatrix} \mathbf{d} = \begin{Bmatrix} \mathbf{f} \\ \mathbf{0} \end{Bmatrix} \tag{23}$$

where the vector of unknown variables $\mathbf{d}$ is including displacement and pressure vector. And

$$\begin{aligned} &\mathbf{A} = 2\mu \int_\Omega \mathbf{B}^T \mathbf{D}_{dev} \mathbf{B} \mathrm{d}\Omega, \quad \mathbf{G} = \int_\Omega \mathbf{B}^T \mathbf{m} \mathbf{N}_p \mathrm{d}\Omega \\ &\mathbf{V} = \frac{1}{\lambda} \int_\Omega \mathbf{N}_p^T \mathbf{N}_p \mathrm{d}\Omega, \mathbf{f} = \int_\Omega \mathbf{N}_u^T b \mathrm{d}\Omega + \int_{\Gamma_t} \mathbf{N}_u^T t_\Gamma \mathrm{d}\Gamma \end{aligned} \tag{24}$$

Note that as $\nu = 0.5, \lambda = \infty$, matrix $\mathbf{V} = \mathbf{0}$, Eq. (23) becomes the form describing the stationary Stokes problem [15].

4. NUMERICAL RESULTS

4.1. Error norm

To evaluate the present method, the quantitative study of the error and convergence rate with three types of error norms [1] (i.e, displacement error norm, pressure error norm and energy error norm) are used.

– The displacement error norm is defined by

$$\begin{aligned} \|\mathbf{u}\| =& \sqrt{\int_\Omega \left(\mathbf{u} - \mathbf{u}^h\right)^T \left(\mathbf{u} - \mathbf{u}^h\right) \mathrm{d}\Omega} = \left(\sum_{e=1}^{nel} \int_{\Omega_e} \left(\mathbf{u} - \mathbf{u}^h\right)^T \left(\mathbf{u} - \mathbf{u}^h\right) \mathrm{d}\Omega \right)^{1/2} \\ =& \left(\sum_{e=1}^{nel} \sum_{i=1}^{n_{GP}} \left(\mathbf{u}_i - \mathbf{u}_i^h\right)^T \left(\mathbf{u}_i - \mathbf{u}_i^h\right) w_i \left|\mathbf{J}\right| \right)^{1/2} \end{aligned} \tag{25}$$

where $\mathbf{u}$ and $\mathbf{u}^h$ are the exact and approximated displacements, respectively, and n_{GP}, w_i are the number and the weight of Gauss points. The Jacobian matrix is expressed as

$$\mathbf{J} = \begin{bmatrix} x_{,\xi} & y_{,\xi} \\ x_{,\eta} & y_{,\eta} \end{bmatrix} \tag{26}$$

– The pressure error norm is given by

$$\|p\| = \left(\sum_{e=1}^{nel} \int_{\Omega_e} \left(p_r - p_r^h\right)^2 \mathrm{d}\Omega \right)^{1/2} = \left(\sum_{e=1}^{nel} \sum_{i=1}^{n_{GP}} \left(p_{ri} - p_i^h\right)^2 w_i \left|\mathbf{J}\right| \right)^{1/2} \tag{27}$$

where p_r and p^h are the analytical and numerical pressure solutions, respectively.

– The last one is used to compute the energy error norm

$$\begin{aligned}\|\mathbf{e}\| =& \sqrt{2\mu \int_{\Omega} (\boldsymbol{\varepsilon} - \boldsymbol{\varepsilon}^h)^T (\boldsymbol{\varepsilon} - \boldsymbol{\varepsilon}^h)\, \mathrm{d}\Omega + \int_{\Omega} (p_r - p_r^h)\mathbf{m}^T (\boldsymbol{\varepsilon} - \boldsymbol{\varepsilon}^h)\, \mathrm{d}\Omega} \\ =& \left(\sum_{e=1}^{nel} \sum_{i=1}^{n_{GP}} \left[2\mu \left(\boldsymbol{\varepsilon}_i - \boldsymbol{\varepsilon}_i^h \right)^T \left(\boldsymbol{\varepsilon}_i - \boldsymbol{\varepsilon}_i^h \right) + \left(p_{ri} - p_i^h \right) \mathbf{m}^T \left(\boldsymbol{\varepsilon}_i - \boldsymbol{\varepsilon}_i^h \right) \right] w_i \, |\mathbf{J}| \right)^{1/2} \end{aligned} \tag{28}$$

in which $\boldsymbol{\varepsilon}$ is the exact strain and $\boldsymbol{\varepsilon}^h$ is derived from Eq. (21).

4.2. Inf-sup test

To qualify the performance of a mixed formulation, besides examining the accuracy and convergence rate of the solutions, it is worth emphasizing that the inf-sup conditions must be verified. In this example, we illustrate three NURBS elements using C^0 continuous derivative of basis functions: quadratic ($p = 2$), cubic ($p = 3$) and quartic ($p = 4$). Fig. 6 shows a numerical study of inf-sup condition for Cook's membrane [16]. This figure describes the relationship of inf-sup value – the smallest nonzero eigenvalue [17] and the total number of NURBS elements N. We can see that as N increases, the logarithm of inf-sup value is almost not change. It is proved that the present elements pass the LBB-condition.

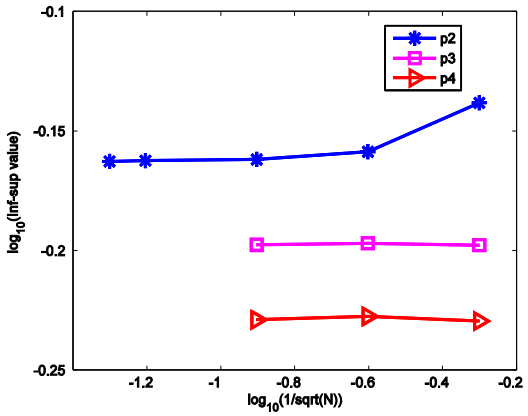

Fig. 6. Numerical inf-sup test for the Cook's membrane

4.3. Steady-state Stokes problem

Next, we consider a 2D cavity problem with the material properties assumed to be fully incompressible ($\nu = 0.5$) and unit viscosity (elastic shear modulus $\mu = 0.5$) [15]. Because of homogeneous Dirichlet condition on the domain boundary, zero constraints are imposed directly for unknown variables at control points on the boundary edges. The convergence norm results for displacement and pressure are plotted in Fig. 7. Here, two kinds of NURBS C^0 continuity elements: quadratic ($p = 2$) and cubic ($p = 3$) element are illustrated to compared with MINI element [9] which displacement (or velocity) field is supplemented with cubic bubble function placed at an additional node in the centroid

of each three-node triangle element. It can be observed that, NURBS elements achieve optimal convergence rate and the cubic element shows the super-convergence in pressure error norm. For illustration, we plot the pressure field and the level line of the velocity field using the quadratic element as shown in Fig. 8. Because of satisfaction LBB condition, this element exhibits the smooth pressure field according to parabolic curved surface as same as analytical solution in [15].

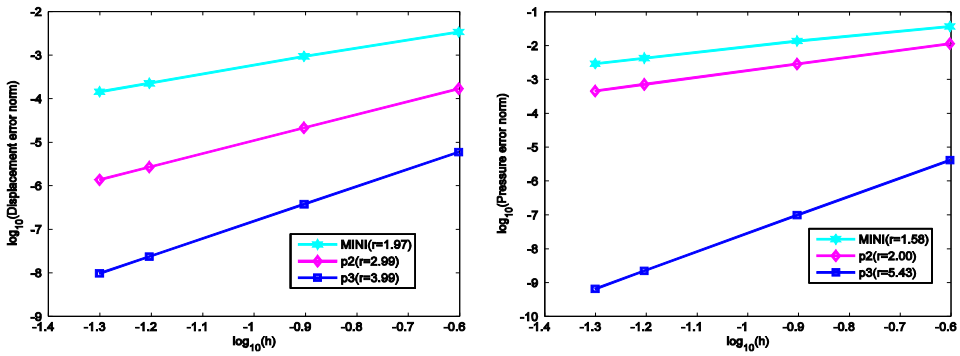

(a) (b)

Fig. 7. Error norm for Stokes problem
(a) displacement error norm, (b) pressure error norm

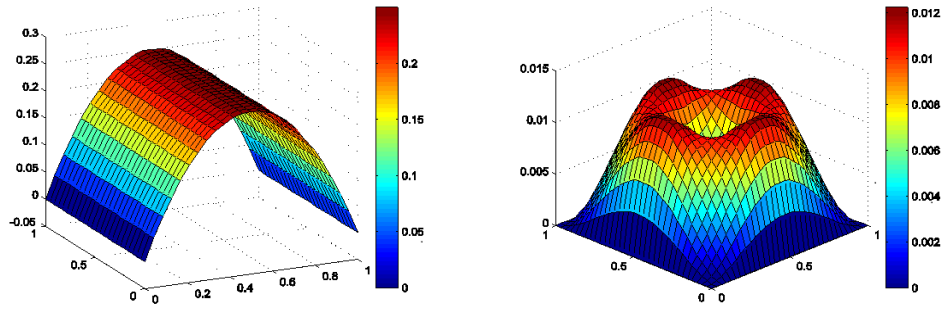

(a) (b)

Fig. 8. Stokes problem: (a) pressure field, (b) level line of $\left(u_x^2 + u_y^2\right)^{1/2}$

4.4. Cylindrical pipe

Finally, let's consider a cylindrical pipe with internal radius $a = 1\,\mathrm{m}$ and external radius $b = 2\,\mathrm{m}$, subjected to an internal pressure $p = 8\,\mathrm{kN/m^2}$ as shown in Fig. 9. Due to the axis-symmetric characteristic of the problem, only the upper right quadrant of the pipe is modelled. Plane strain condition is assumed and Young's modulus is $E = 21000\,\mathrm{kN/m^2}$

and Poisson's ratio is $\nu = 0.5$. Symmetric conditions are imposed on the left and bottom edges, and the outer boundary is traction free. The exact solution for the radial and tangential exact displacements [18] are expressed as

$$u_r(r) = \frac{(1+\nu)a^2 p}{E(b^2-a^2)}\left\{(1-2\nu)r + \frac{b^2}{r}\right\} \quad ; \quad u_\varphi = 0 \tag{29}$$

and the radial and tangential exact stresses are given by

$$\sigma_r(r) = \frac{a^2 p}{b^2-a^2}\left(1-\frac{b^2}{r^2}\right); \quad \sigma_\varphi(r) = \frac{a^2 p}{b^2-a^2}\left(1+\frac{b^2}{r^2}\right); \quad \sigma_{r\varphi} = 0 \tag{30}$$

where (r, φ) are the polar coordinates, and φ is measured counter-clockwise from the positive x-axis.

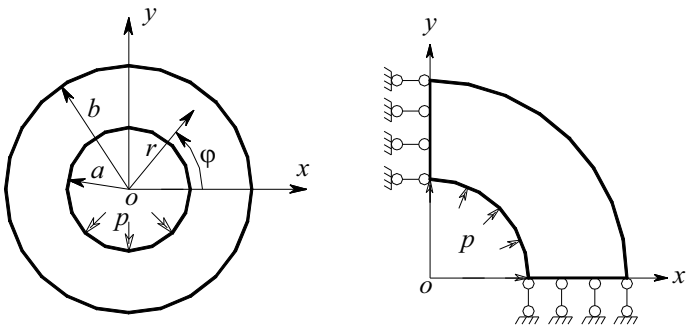

Fig. 9. A cylindrical pipe subjected to an inner pressure and its quarter model with symmetric conditions imposed on the left and bottom edges

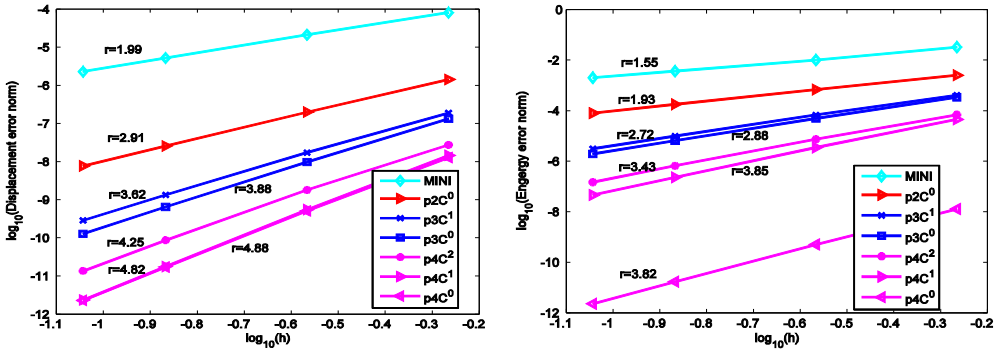

(a) (b)

Fig. 10. Error norm for cylindrical pile
(a) displacement error norm, (b) energy error norm

Here, we coin a family of NURBS elements marked by piC^k. It means that the displacement field is approximated with NURBS basis functions having the order $p = i$ and the pressure field has the order $p = i - 1$ and both are C^k continuous derivative.

The convergence of displacement and energy error norms are displayed in Fig. 10. The general observations are found that (1) results of the present elements are more accurate and convergent than that of the MINI [9] derived from the FEM; (2) with the same used elements, the obtained solutions are more and more accurate as p increases. The convergence rate is about from 2.91 to 3.88, 4.82 for displacement norm and from 1.93 to 2.88, 3.82 for energy norm according to $p = 2$, 3, 4, respectively; (3) with the same approximated order, C^0 continuity elements produce the best results compared to the counterparts.

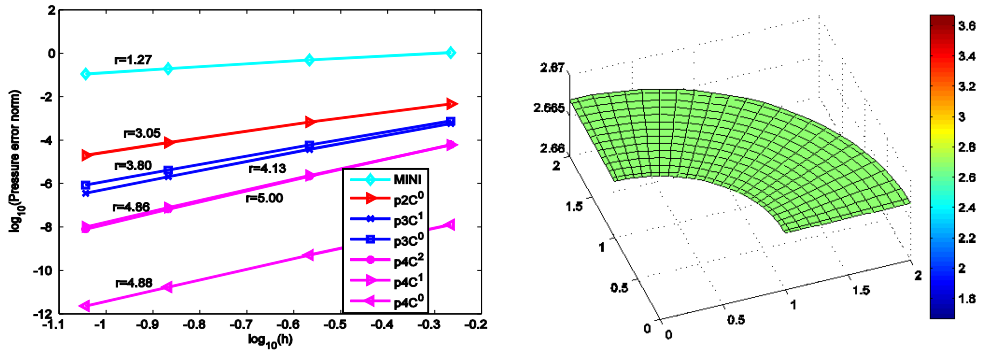

(a) (b)

Fig. 11. Cylindrical pipe problem: (a) pressure error norm, (b) pressure field

Again conclusions are observed in Fig. 11a for pressure error norm of cylindrical pipe problem. Fig. 11b reveals the pressure field computed by NURBS elements. The pressure is constant over the problem domain with the approximate value of 2.66.

5. CONCLUSION

In this paper, we utilized NURBS basis functions to construct **u**-p mixed formulation. By choosing order and continuous derivative of interpolated functions, we have established a family of NURBS elements which satisfies the inf-sup condition. Two benchmark numerical examples including: steady-state Stokes problem and cylindrical pile showed that the present elements are superior to the well-known MINI that is derived from the FE formulation. The present method can produce uniform and optimal convergence rates in displacement, energy and pressure norms. Furthermore, the obtained pressure field is stable with no spurious mode. The method is thus promising to apply for incompressible Navier – Stokes fluid flows.

ACKNOWLEDGEMENT

This research is funded by Vietnam National University Ho Chi Minh City (VNU-HCM) under grant number B2013-18-04. The support is gratefully acknowledged.

REFERENCES

[1] O.C. Zienkiewicz, R.L. Taylor, *The Finite element method*, fifth ed. (vol.1), Butterworth Heinemann, Oxford, (2000).

[2] F. Brezzi, M. Fortin, *Mixed and hybrid finite element methods*, Springer-Verlag, New York, (1991).

[3] J.C. Simo, M.S. Rifai, A class of mixed assumed strain methods and the method of incompatible modes, *International Journal for Numerical Methods in Engineering*, **29**, (1990), pp. 1595–1638.

[4] T. Belytschko, L.P. Bindeman, Assumed strain stabilization of the 4-node quadrilateral with 1-point quadrature for nonlinear problems, *Computer Methods in Applied Mechanics and Engineering*, **88**(3), (1991), pp. 311–340.

[5] J. Bonet, A.J. Burton, A simple average nodal pressure tetrahedral element for incompressible and nearly incompressible dynamic explicit applications, *Communications in Numerical Methods in Engineering*, **14**(5), (1998), pp. 437–449.

[6] A. Huerta, S. Fernandez-Mendez, Locking in the incompressible limit for the element free-Galerkin method, *International Journal for Numerical Methods in Engineering*, **51**(11), (2001), pp. 1361–1383.

[7] C.T. Wu, W.Hu, Meshfree-enriched simplex elements with strain smoothing for the finite element analysis of compressible and nearly incompressible solids, *Computer Methods in Applied Mechanics and Engineering*, **200**, (2011), pp. 2991–3010.

[8] A.J. Chorin, A numerical method for solving in compressible viscous problems, *J. Comput. Phys.*, **2**(1), (1967), pp. 12–26.

[9] D. Arnold, F. Brezzi, M. Fortin, A stable finite element for the Stokes equations, *Calcolo* , **21**(4), (1984), pp. 337–344.

[10] T.J.R. Hughes, J.A. Cottrell, and Y. Bazilevs, Isogeometric analysis: CAD, finite elements, NURBS, exact geometry and mesh refinement, *Computer Methods in Applied Mechanics and Engineering*, **194**(39), (2005), pp. 4135–4195.

[11] J.A. Cottrell, T.J.R. Hughes, Y. Bazilevs, Isogeometric analysis, Toward Integration of CAD and FEA, Wiley, (2009).

[12] T.E lguedj, Y. Bazilevs, V. Calo, T. Hughes, B-bar and F-bar projection methods for nearly incompressible linear and non-linear elasticity and plasticity using higher-order NURBS elements, *Computer Methods in Applied Mechanics and Engineering*, **197**, (2008), pp. 2732–2762.

[13] A. Buffa, C. de Falco, G. Sangalli, Isogeometric analysis: stable elements for the 2D Stokes equation, *Int. J. Numer. Methods Fluids*, **65**(11-12), (2011), pp. 1407–1422.

[14] P. N. Nielsen, R. Gersborg, J. Gravesen, N. L. Pedersen, Discretizations in isogeometric analysis of Navier–Stokes flow, *Comput. Methods Appl. Mech. Engrg*, **200**, (2011), pp. 3242–3253.

[15] A. Huerta, *Finite element methods for flow problems*, John Wiley & Sons, Ltd, (2003).

[16] R. Cook, Improved two-dimensional finite element, *Journal of the Structural Division* (*ASCE*), **100**(9), (1974), pp. 1851–1863.

[17] A. Ortiz, M.A. Puso, N. Sukumar, Maximum-entropy mesh free method for incompressible media problems, *Finite Elements in Analysis and Design*, **47**(6), (2011), pp. 572–585.

[18] S.P. Timoshenko, J.N. Goodier, *Theory of elasticity (3rd edn)*, McGraw-Hill, New York, (1970).

Received May 25, 2012

VIETNAM ACADEMY OF SCIENCE AND TECHNOLOGY
VIETNAM JOURNAL OF MECHANICS VOLUME 35, N. 3, 2013

CONTENTS

Pages